

The 21cm Absorption Line and the Axion Quark Nugget Dark Matter Model

K. Lawson and A.R. Zhitnitsky

Department of Physics & Astronomy, University of British Columbia, Vancouver, B.C. V6T 1Z1, Canada

Abstract

We argue that dark matter in the form of macroscopically large nuggets of standard model quarks and antiquarks can help to alleviate the tension between standard model cosmology and the recent EDGES observation of a stronger than anticipated 21 cm absorption feature. The effect occurs as a result of the thermal emission from quark nugget dark matter at early times and at energies well below the peak of the CMB. Similar radiation at early times may also contribute a fraction of the GHz range excess observed by ARCADE2.

1. Introduction

Redshifted 21 cm emission serves as a tracer of baryonic physics in the early universe prior to reionization. Observations by the low-band antenna of the Experiment to Detect the Global EoR Signal (EDGES) of a stronger than anticipated 21 cm absorption feature pose a challenge to our standard picture of the early universe [1]. This signal suggests a larger than expected difference between the radiation temperature and the spin temperature of the absorbing hydrogen gas. In particular it has been suggested that a stronger than expected radio background present at $z > 17$ may be capable of producing the EDGES result [2]. The possibility of a low energy excess was also indicated by the earlier observations of ARCADE2 in the GHz range [3] but at a level significantly above that required to produce the EDGES feature.

The EDGES result has sparked a number of proposals designed to alleviate its tension with the standard cosmological framework. In particular, it has been suggested that the dark matter (DM) may act as a heat sink cooling the neutral gas relative to the CMB [4–8]. However this idea seems to be subject to several very strong constraints [9–13] and may be inconsistent with results from the CMB and Lyman-alpha flux [14].

Another proposal to ease the tension with the conventional model is to introduce an additional source of soft radiation at large redshifts ($z \gtrsim 17$)

as suggested in [15] using DM particles [16, 17] or intermediate mass black holes as suggested in [18]. However, models in which dark matter or black holes are capable of modifying the soft photon spectrum generally also modify the hard photon spectrum, which is strongly constrained by independent observations. Therefore, any model introduced to explain the EDGES result must produce emission which is strongly suppressed at energies above the radio band. Additionally, synchrotron production of the required soft photon background is disfavoured by the relatively short cooling time of synchrotron emitting astrophysical electrons [19]. Alternatively it has been suggested that a different choice of foreground parameters than those used in [1] may give very different properties of the absorption profile [20].

Here we present a proposal which may remove the tensions related to the EDGES results as highlighted above. The arguments are based on the Axion Quark Nugget (AQN) dark matter model. This model was originally invented as an explanation of the observed similarity in the visible and dark matter densities

$$\Omega_{\text{dark}} \sim \Omega_{\text{visible}} \quad (1)$$

as it naturally produces these components at the same scale independent of the specific values of any of the parameters of the model. We overview the basic ideas of this model in section 2 but first make two important comments related to this model in

the context of the present work.

First, the AQN model was invented long ago [21], though a specific formation mechanism for the nuggets has been developed in the much more recent papers [22–24]. It was proposed independently of the recent EDGES observations [1] and, in contrast with much recent activity in the field, the AQN model was not invented specifically to explain the EDGES result. Rather, this model was invented as a natural explanation of the observed dark matter to baryon ratio of expression (1). The similarity between the dark matter Ω_{dark} and the visible matter Ω_{visible} densities strongly suggests that both types of matter formed during the same cosmological epoch. For the baryon density this is obviously the QCD phase transition as the baryon mass m_p is proportional to Λ_{QCD} while the electroweak contribution proportional to the quark masses m_q represents only a minor contribution to the baryon mass.

The second comment we would like to make in this Introduction is as follows. Observations made by ARCADE2 in the GHz range [3] hinted at a possible excess of diffuse radiation. The authors of [2] argue that just $\sim 1\%$ of this excess is needed to explain the EDGES result. We have previously argued in [25] that the AQN model will necessarily contribute to the radio background across a broad range from the MHz up to the GHz scale, though a precise computations within AQN model are hard to carry out due to very high sensitivity to some unknown parameters. However, the main conclusion of [25] holds in a sense that the AQN model offers a potential mechanism to generate the soft photon background assumed to be present in [2] and capable of producing the EDGES result.

At this time the EDGES result seems to indicate that the dominant contribution to ARCADE2 cannot be associated with any excess prior to $z \sim 20$ as it would overproduce the observed absorption feature. Instead, only a small portion about 1% of the ARCADE2 excess is consistent with EDGES result, which we assume to be the case.

Our presentation is organized as follows. In Section 2 we provide an overview of the AQN dark matter model with emphasis on cosmological and astrophysical implications. In section 3 we discuss some specific features of the spectrum radiated by the nuggets at large z . In Section 4 we compute the resulting sky temperature and argue that recent EDGES observations can be understood within the AQN framework.

2. Axion Quark Nugget dark matter model

The idea that the dark matter may take the form of composite objects composed of standard model quarks in a novel phase goes back to quark nuggets [26], strangelets [27] and nuclearities [28], for a large number of references to these original results see the review [29]. In the models of [26–29] the presence of strange quarks stabilizes quark matter at sufficiently high densities allowing strangelets formed in the early universe to remain stable over cosmological timescales. There were however a number of problems with the original model which shall not be discussed here¹.

The AQN model [21] is so named in order to emphasize the essential role of the axion field in its construction and to avoid confusion with the earlier models [26–29] mentioned above. It is drastically different from the previous proposals in two key aspects:

1. There is an additional stabilization factor in the AQN model provided by the axion domain walls which are copiously produced during the QCD transition, such that a first order QCD phase transition as mentioned in footnote 1 is not required.
2. The AQN could be made of matter as well as *antimatter* in this framework as a result of separation of charges. Precisely this feature plays a key role in the context of the present work.

The basic idea of the AQN proposal can be explained as follows: It is commonly assumed that the Universe began in a symmetric state with zero global baryonic charge and later (through some baryon number violating process, the so-called baryogenesis) evolved into a state with a net positive baryon number. As an alternative to this scenario we advocate a model in which “baryogenesis” is actually a charge separation process in which the global baryon number of the Universe remains zero. The baryon to photon ratio $\eta = n_B/n_\gamma \sim 10^{-10}$ is determined by the formation temperature $T_{\text{form}} \simeq 40$ MeV when the nuggets complete their formation. The AQN framework is very different from the conventional baryogenesis mechanism in which

¹In particular, a first order phase transition is required for the strangelets to be formed during the QCD phase transition. However recent lattice results [30] unambiguously show that the QCD transition is a crossover rather than a first order phase transition. Furthermore, the strangelets will likely evaporate on the Hubble time-scale even if they had been formed [31].

a single extra baryon must be produced for every 10^{10} particles in the primordial plasma.

In this model the unobserved baryons and antibaryons locked in the nuggets come to comprise the dark matter in the form of quarks and antiquarks in a dense colour superconducting (CS) phase. The formation of the nuggets made of matter and antimatter occurs through the dynamics of shrinking axion domain walls. For technical details of the formation process which will only be briefly discussed here see the recent original papers [22–24].

The nuggets are originally compressed by the collapse of an axion domain wall at the time of the QCD transition. With the domain wall collapsing until it is countered by the fermi pressure of the quarks inside. Consequently they have a typical size $R \sim (10^{-5} - 10^{-4})$ cm determined by the axion mass m_a with $R \sim m_a^{-1}$. It is important to emphasize that there are strong constraints on the allowed window for the axion mass, which can be represented as follows $10^{-6}\text{eV} \leq m_a \leq 10^{-2}\text{eV}$, see recent reviews [32–40] on the subject. The Compton wavelength of the axion represents that largest scale in the AQN formation process and consequently sets a maximum baryon number for the nuggets $B^{1/3} \lesssim \frac{m_\pi}{m_a}$ [24] strongly limiting the parameter space in which the AQN model may be stable and comprise the dark matter. It is a highly nontrivial self-consistency check of this model that the axions search constraints on m_a and independent constraints on the mass of the nuggets $\mathcal{M} \simeq Bm_p$ are overlapping as we review below.

At temperatures below the QCD phase transition the quarks (in the nuggets) or antiquarks (in the antinuggets) inside a closed axion wall cool and settle into a high density colour superconducting phase [22]. It is the degeneracy pressure of this state which supports the domain wall against further collapse. Under the conditions considered here this pressure is significantly larger than the thermal pressure inside the domain wall. At asymptotically large densities the ground state would contain an equal number of u, d and s quarks (the so called CFL phase) while at lower densities s quarks are relatively depleted due to their larger mass. The resulting combination of u and d quarks is electrically charged, positive in the case of quark matter and negative in the case of antiquarks. There is thus a strong electrical potential surrounding the nuggets which rapidly results in the formation of a surrounding layer of leptons (captured from the sur-

rounding primordial plasma) electrons in the case of a quark nugget and positrons in the case of an antiquark nugget. This lepton layer is known as the electrosphere and largely determines the observable properties of the nuggets. The emergence of the electrosphere characterized by the chemical potential μ is not a specific feature of the AQNs, rather it is a generic property of all quark nugget models [26–29]. While the details of the interaction between the electrosphere and the surrounding plasma are highly complicated the majority of the leptons are in tightly bound $\mu \sim 10\text{MeV}$ states so that their interactions are suppressed when $T < 1\text{MeV}$. The electrosphere is capable of emitting photons with sufficient efficiency that nuggets may be cold relative to the background plasma for much of their existence. For further details on the low temperature structure of the electrosphere when the core of the nuggets is in a CS phase see [41].

The allowed mass of the AQN is constrained by a variety of direct and indirect observational constraints. As the AQN are strongly interacting searches constrain their number density rather than interaction strength, consequently they impose constraints on,

$$n_N = \frac{\rho_{DM}}{\langle \mathcal{M} \rangle} \approx \frac{\rho_{DM}}{m_p \langle B \rangle} \quad (2)$$

where $\langle \mathcal{M} \rangle$ is the average mass of the nuggets and $\langle B \rangle$ is their average baryon number, not to be confused with the baryon number B of individual nuggets, see (6) below. The low mass regime is strongly constrained by a variety of direct searches [42, 43] requiring

$$\langle \mathcal{M} \rangle \gtrsim 10^{-2}\text{kg}, \quad |\langle B \rangle| \gtrsim 10^{25}, \quad (3)$$

while some individual nuggets could have much lower baryon charge $B \ll 10^{25}$ as discussed below.

Lensing constraints apply at higher masses but only above the region favoured by the allowed axion mass range [42]. Lunar seismology also limits the fraction of the nugget population that falls in the mass range 10 kg - 1000 kg ($10^{28} \lesssim |B| \lesssim 10^{30}$) to account for less than 10% of the local dark matter flux [44]. This result is however sensitive to the efficiency with which the nuggets couple to long wavelength seismic waves. Limits on the contribution of antiquark nugget annihilations to earth heating also limit the the mean baryon charge of the nuggets to $\langle B \rangle > 3 \times 10^{24}$ [45], consistent with the constraint (3).

This model is perfectly consistent with all known astrophysical, cosmological, satellite and ground based constraints within the parametrical range for the mass $\langle M \rangle$ and the baryon charge $\langle B \rangle$ given by (3). It is also consistent with known constraints from the axion search experiments. Furthermore, there are a number of frequency bands where some excess of emission was observed, but not fully explained by conventional astrophysical sources. Our comment here is that this model may explain some portion, or even the entire excess of the observed radiation in these frequency bands, see the short review [43] and additional references at the end of this section.

Another key element of this model is the coherent axion field θ which is assumed to be non-zero during the early Universe QCD transition. As a result of these \mathcal{CP} violating and non-equilibrium processes the number of nuggets and antinuggets formed will be different. This difference is always an order one effect [22–24] irrespective of the parameters of the theory, the axion mass m_a or the initial misalignment angle θ_0 . This disparity between nugget and antinugget formation produces a similar disparity between visible quarks and antiquarks. This is precisely the reason the resulting visible and dark matter densities must be the same order of magnitude: they are both proportional to the same fundamental Λ_{QCD} scale and they both are originated at the same QCD epoch resulting in the relation in expression (1). If these processes are not fundamentally related then the two components Ω_{dark} and Ω_{visible} could easily exist at vastly different scales.

If we assume that the quark nuggets explain the entirety of both the baryon asymmetry and the dark matter then the matter component of the universe consists of antiquark nuggets with mass density $\rho_{\bar{N}}$, quark nuggets with mass density ρ_N and free baryons with mass density ρ_B in the approximate ratio

$$\rho_{\bar{N}} : \rho_N : \rho_B \simeq 3 : 2 : 1, \quad (4)$$

which corresponds to a zero total baryon charge of the Universe, while the ratio of the visible to DM densities $\rho_{DM} = (\rho_N + \rho_{\bar{N}})$ takes the observed value of $\rho_B / (\rho_N + \rho_{\bar{N}}) \sim 1/5$. For a more quantitative treatment of this problem accounting for slight differences between energy densities in the hadronic (for baryons) and CS (for nuggets) phases and the presence of the propagating dark matter axions contributing to ρ_{DM} see [24].

Unlike conventional dark matter candidates, such as Weakly Interacting Massive Particles (WIMPs) the AQN are strongly interacting and macroscopically large objects. However, they do not contradict the many known observational constraints on dark matter or antimatter in the Universe for the following main reasons [46]: They carry a very large baryon charge $\langle B \rangle \gtrsim 10^{25}$, and so their number density is very small $\sim B^{-1}$. As a result of interactions scaling with area, while number density is inversely proportional to the volume the small cross-section to mass ratio replaces the conventional WIMP requirement of weak interaction. In other words, their interaction with visible matter is highly inefficient, and therefore, the nuggets are perfectly qualified as dark matter candidates. They do not contradict conventional CMB results due to the same unique feature. Furthermore, the quark nuggets have a very large binding energy due to the large gap $\Delta \sim 100$ MeV in the CS phases. Therefore, the baryon charge is so strongly bound in the core of the nugget that it is not available to participate in big bang nucleosynthesis at $T \sim 100$ keV, long after the nuggets have been formed². This large gap also prevents non-relativistic protons from easily penetrating into the nugget slowing the rate at which visible matter will annihilate with the antiquark nuggets at late cosmological times. Annihilation is a complicated process accompanied by a strong suppression factor which itself varies depending on the temperature, density and ionization of the surrounding environment in a non-trivial way.

It should be noted that the galactic spectrum contains several excesses of diffuse emission the origin of which is unknown, the best known example being the strong galactic 511 keV line. The rare annihilation of the antimatter contained in an AQN with galactic visible matter could offer a potential source for several of these diffuse components (including the 511 keV line [48, 49] and accompanying continuum of γ rays in the 100 keV to MeV range [41, 50], as well as x-rays [51], and radio frequency bands [52]). It is important to emphasize that all

²While the AQN model basically does not modify the production of the dominant elements such as hydrogen, helium and deuterium with $Z \leq 2$ as mentioned above, it may suppress the production of subdominant heavy nuclei with high $Z \geq 3$ due to the strong Boltzmann factor $\exp(-Z)$ as argued in [47]. Within AQN framework this represents a possible resolution of the primordial ${}^7\text{Li}$ puzzle in which conventional computations predict a higher value for the ${}^7\text{Li}$ abundance in comparison with observations.

these emissions at drastically different frequencies scale with a single fundamental parameter of the model, the average baryon charge of the nugget $\langle B \rangle$, or equivalently, the axion mass m_a . This is because the rate of annihilation events is proportional to one and the same product of the local visible and DM distributions at the annihilation site defined as

$$\Phi \sim 4\pi R^2 \int d\Omega dl [n_{\text{visible}}(l) \cdot n_{DM}(l)], \quad (5)$$

where $R^2 \sim B^{2/3}$ is the effective cross section σ of interaction between the AQN and visible matter. As $n_{DM} \sim \mathcal{M}^{-1} \sim B^{-1}$ the effective interaction (5) is strongly suppressed $\sim B^{-1/3} \ll 1$. Precisely this small geometrical factor replaces the conventional WIMPs requirement for weakness of the dark-visible coupling. The AQNs achieved this weakness not as a result of a new fundamental weak coupling constant but rather through suppression as a result of large baryon number B constrained by eq. (3).

To conclude our brief review of the AQN model we would like to mention the recent claim [53–55] that the AQNs might be responsible for the resolution of the renowned (since 1939) “solar corona heating mystery”. The puzzle is that the corona has a temperature $T \simeq 10^6\text{K}$ which is 100 times hotter than the surface temperature of the Sun, and conventional astrophysical sources fail to explain the extreme UV (EUV) and soft x ray radiation from the corona 2000 km above the photosphere.

It turns out that if one estimates the extra energy being injected when the antiquark nuggets annihilate with the solar material one obtains a total extra energy $\sim 10^{27}\text{erg/s}$ which automatically reproduces the observed EUV and soft x-ray energetics [53]. This estimate is derived exclusively in terms of known dark matter density $\rho_{DM} \sim 0.3 \text{ GeVcm}^{-3}$ and dark matter velocity $v_{DM} \sim 10^{-3}c$ surrounding the Sun without adjusting any parameters of the model. This estimate is strongly supported by Monte Carlo numerical computations [54] which suggest that most annihilation events occur precisely at the so-called transition region at an altitude of 2000 km, where it is known that drastic changes in temperature and density occur.

A “smoking gun” supporting this proposal on the nature of the EUV would be the observation of axions radiated from the corona when the nuggets disintegrate in the Sun. The corresponding computations have been carried out recently in [56, 57]. Presently the CAST (CERN Axion Search Tele-

scope) Collaboration has taken a significant step to upgrade its instrument to make it sensitive to the spectral features of the axions produced due to the AQN annihilation events on the Sun.

In the context of this work it is important to emphasize that this picture when the AQNs are responsible for the resolution of the “solar corona heating mystery” is consistent with the old idea advocated by Parker [58] suggesting that there must be small, sub-resolution events, the so-called “nanoflares”, which uniformly heat the corona. In most studies the term “nanoflare” describes a generic burst-like event for any impulsive energy release on a small scale, without specifying its cause, the hydrodynamic consequences of impulsive heating are assumed without discussing their nature, see the recent review papers [59, 60]. The AQN framework offers a specific realization of these nanoflares in form of the AQN annihilation events, see [53–55] with details and references on the original literature on observations supporting this identification. This identification implies that the baryon number distribution must be in the range

$$10^{23} \leq |B| \leq 10^{28}. \quad (6)$$

It is a highly nontrivial consistency check for the proposal [53–55] that the required window (6) is consistent with the range of mean baryon number allowed by the axion and dark matter search constraints (3) as these come from a number of different and independent constraints extracted from astrophysical, cosmological, satellite and ground based observations. It is this range of AQN masses which will be used in our estimates of their contribution to the background sky temperature in Section 4.

3. Thermal Radiation from Nuggets

The AQNs begin as cold objects as the initial heat of formation will be quickly released as radiation from the electrosphere as will be discussed below. The quark nuggets may be cold relative to the photon background because the electrosphere is characterized by a plasma frequency (ω_p) which prevents the photons from outside penetrating into the nuggets’ interior and efficiently depositing heat [52].

While photon heating is very inefficient the antiquark nuggets are heated through interactions with the surrounding visible matter as a result of annihilation events in their interior. This heating results in radiation which depends on environment: a

denser environment leads to more annihilations, a higher temperature and stronger radiation from the AQNs. Of particular importance is the fact that the nuggets emit a non-black body spectrum which will distort the low energy CMB spectrum³. The spectrum of nuggets at low temperatures was analyzed in [52] and was found to be,

$$\frac{dE}{dt d\nu dA} = \frac{32\pi^2}{45} \frac{\alpha^{5/2} (k_B T_N)^3}{(hc)^2} \sqrt[4]{\frac{k_B T_N}{m_e c^2}} \times \left(1 + \frac{h\nu}{k_B T_N}\right) e^{-h\nu/k_B T_N} F\left(\frac{h\nu}{k_B T_N}\right) \quad (7)$$

where T_N is the nuggets' effective radiating temperature, m_e is the electron mass and we have defined the function,

$$F(x) = 17 - 12\ln\left(\frac{x}{2}\right) \quad x < 1, \quad (8)$$

$$= 17 + 12\ln(2) \quad x > 1$$

to simplify notation. The spectrum (7) is very hard at low frequencies $\nu \ll T_N$ relative to black body radiation which will play an important role in our analysis. While it is not relevant at the energies considered here the spectrum in equation (7) has a low energy cutoff due to finite size effects within the electrosphere. As discussed in [25] this effect strongly suppresses the present day radio background below ~ 10 MHz.

The total energy emitted by the nugget per unit time per unit area dA is given by integrating expression (7) over all emission frequencies to obtain,

$$\frac{dE}{dt dA} = \frac{128\pi^2}{3} \frac{\alpha^{5/2} (k_B T_N)^4}{h^3 c^2} \sqrt[4]{\frac{k_B T_N}{m_e c^2}}. \quad (9)$$

The corresponding intensity is almost 6 orders of magnitude smaller than black body radiation for temperatures at the eV scale. The nuggets are therefore very inefficient emitters at the time of CMB formation and do not distort the conventional CMB results⁴. However, the low energy tail (which

³The spectrum of the nuggets is determined by emission of photons in the electrosphere with temperature T_N and deviates from black body radiation as discussed in [52]. In particular, at low energies the spectrum is logarithmic $dE/d\nu \sim \ln \nu$ in contrast with black body radiation $dE/d\nu \sim \nu^2$. Some additional constraints on the low energy tail emerge as a result of finite size effects of the electrosphere relative to the wavelength of the emitted photons.

⁴Nevertheless, this rate of emission is fast compared with cooling rate of CMB radiation due to the Universe's expansion and the nuggets' temperature would drop very fast, in a matter of seconds, if annihilation events heating the nuggets were not happening.

scales as $\sim \ln \nu$) of the emission from the nuggets is drastically different from black body radiation ν^2 . This observation will play a key role in our arguments which follow.

As argued above the AQNs are not effectively heated by the relatively low energy photons of the radiation background. As such the nuggets composed of quarks will have a temperature well below the radiation. This is not however the case for nuggets composed of antiquarks which may be heated by the capture and annihilation of surrounding matter. If the antiquark nuggets interact sufficiently to be in radiative equilibrium the energy output of expression (9) must be balanced by the rate at which annihilations deposit energy in the AQNs⁵. In particular the energy flux onto an AQN should satisfy,

$$\frac{dE}{dt dA} \propto \rho_{\text{vis}} v \quad (10)$$

such that the nuggets will be warmer in environments with larger visible matter densities and temperatures. If the surrounding environment is sufficiently ionized the energy input may differ from the basic expression (10) due to the influence of long range electromagnetic interactions.

The total amount of energy injected into the plasma is negligibly small and does not modify the conventional cosmological analysis, as argued in the simple estimates in Appendix B. The only comments we will make here is that the observational consequences advocated in this work emerge due to a very specific feature of the low energy spectrum: it scales as $\ln \nu$ in eq. (7) instead of the conventional ν^3 for radiation of a plasma at temperature T . The corresponding portion of the spectrum generates a negligible amount of energy at the moment of emission as stated above. However, this excess becomes important at later times as it is redshifted across the 21 cm transition as a result of expansion as will be discussed in section 4.

The radiating temperature of the nuggets will evolve with redshift following a power law of the form

$$T(z) = T_{\text{rec}} \left(\frac{1+z}{1+z_{\text{rec}}} \right)^\beta \quad (11)$$

⁵While the majority of energy deposited in the nugget fully thermalizes some small amount will be emitted at higher energies. The resulting cosmic background also produces a constraint on the AQN model but it is considerably weaker than the effects discussed here. See appendix Appendix A for further details.

where $z_{\text{rec}} \approx 1100$ is the redshift at recombination and T_{rec} is the nuggets' average radiative temperature at that time. We may estimate the power law exponent β by noting that the total thermal emission in expression (9) scales as $T_N^{17/4}$. If the heating is annihilation dominated then the energy input follows equation (10) which scales as $(1+z)^{3.5}$ if the matter is thermally coupled to the CMB or as $(1+z)^4$ if it is cooling adiabatically. These two possible scaling laws would imply either $\beta \approx \frac{14}{17}$ or $\beta \approx \frac{16}{17}$. It should be noted that emission is strongly dominated by the contribution from large z so that the observable spectrum is largely insensitive to the precise value of β . More important is the nuggets' effective radiating temperature at the time the universe first becomes transparent to low energy radiation.

If the nuggets are in radiative equilibrium with the surrounding environment then we expect the radiative output of equation (9) must balanced the rate at which annihilations deposit energy in the nugget according to expression (10). In this case we may write,

$$\frac{128\pi^2 \alpha^{5/2} (k_B T_N)^4}{3 h^3 c^2} \sqrt[4]{\frac{k_B T_N}{m_e c^2}} = \kappa \rho_{\text{vis}} v \quad (12)$$

The factor κ is introduced to account for the fact that collision rate need not strictly match the annihilation rate as not all matter striking the nugget will annihilate and not all of the energy released by an annihilation will be thermalized in the nuggets. As such κ encodes a large number of complex processes including the probability that low momentum protons are unlikely to overcome the larger gap and penetrate into the colour superconducting phase of the nugget as well as charge exchange effects between the hydrogen atom and the nugget. These may involve either the annihilation of the electron or charge exchange between the proton and the central quark matter or interactions with a hole state in the electrosphere. In a neutral environment when no long range interactions exist the value of κ cannot exceed $\kappa \sim 1$ which would correspond to the instantaneous and total annihilation of all impacting matter into thermal photons. The high probability of reflection at the sharp quark matter surface lowers the value of κ while ionization due to electron annihilation increases the value of κ .

Annihilation events are suppressed by a number of complicated many-body effects. In particular, an incoming proton for a successful annihilation must

overcome a sharp boundary between the CS and hadronic phases. Also, a successful annihilation is accomplished only if the quantum numbers of the three quarks of the proton exactly match the quantum numbers of a drastically different di-quark condensate and a quark excitation in CS phase. In addition to these primary suppression mechanisms there are many other many-body effects which must be taken into account for a proper estimation of parameter κ . For that reasons a computations of the parameter $\kappa < 1$ from first principles in strongly coupled QCD is not even feasible at the moment. A determination of κ also depends on the environment and includes accounting for the fraction of annihilation energy lost through non-thermal emission⁶. Given the impracticality of directly calculating the value of κ we will adopt a phenomenological approach in which we determine the value of κ at $z \simeq 17$ consistent with the EDGES observation and then comment on the consistency of this value with physical expectations and with other observational constraints on the model.

We start our task by estimation of the average velocity of the hydrogen. At the time of recombination the photons have a temperature of ≈ 0.3 eV and the neutral hydrogen is expected to follow a Maxwell distribution at this temperature. Consequently the average velocity of the hydrogen is,

$$\langle v \rangle = \sqrt{\frac{8k_B T_\gamma}{\pi m_p}} \approx 9 \times 10^5 \text{ cm/s}. \quad (13)$$

The hydrogen is also very uniformly distributed with a density,

$$\rho_{\text{vis}} = \Omega_B \rho_c (1 + z_{\text{rec}})^3 \approx 330 \frac{m_p c^2}{\text{cm}^3}, \quad (14)$$

where Ω_B is the baryon fraction, ρ_c is the critical density and m_p is the proton mass. Substituting (13) and (14) to (12) we arrive to our estimate for the temperature in terms of unknown parameter κ ,

$$T_{\text{rec}} = 0.7 \text{ eV} \cdot \kappa^{4/17}. \quad (15)$$

It is instructive to compare the obtained estimate (15) with the analogous study of the galactic environment [51, 52] where the internal temperature

⁶Near surface annihilations may result in the emission of both x-rays [52] and charged particles [61]. However the branching fraction to these higher energy products is expected to be small and is constrained by both the cosmic background as discussed in appendix A and by present day observations[62].

of a nugget was estimated on the level $T \simeq 1$ eV. In both cases the numerical values for the densities ρ_{vis} assume the same order of magnitude, while the galactic velocity $\sim 10^{-3}c$ is slightly higher than (13). This leads to numerical similarity between T_{rec} given by (15) and $T \simeq 1$ eV obtained for the galactic environment [51, 52].

It should also be noted that while expression (15) may allow for the AQN to have a temperature comparable to that of the photons they have little impact on the present day CMB as any effects are suppressed by both the baryon to photon ratio (expressed in terms of $\eta \sim 10^{-10}$) and the small cross section to mass ratio of the AQN (represented by parameter $\sigma/M \sim B^{-1/3}$), similar to our estimates of the AQN impact on pre-BBN effects carried out in Appendix B.

We emphasize that the key ingredient generating the observable effect from AQN is the drastic difference in the spectrum in equation (7) with its $\ln \nu$ behaviour in comparison with the conventional black body portion ν^2 of the CMB at low frequencies. These distinct spectral features will play the crucial role in our arguments in the next section.

4. Soft Photon Excess from AQN Dark Matter

As was claimed in [2] a stronger than predicted radiation background present before $z \sim 20$ may produce the strong 21 cm absorption feature observed by EDGES. This results from the larger misalignment between the radiation temperature and the spin temperature of neutral hydrogen with the strength of this feature scaling as,

$$\delta T \sim x_{HI} \left(1 - \frac{T_r}{T_s} \right) \quad (16)$$

where x_{HI} is the fraction of neutral hydrogen and T_r and T_s are the radiation and gas spin temperatures respectively.

In what follows we will demonstrate that the radiation background produced by the nuggets mimics that required to produce the 21 cm absorption strength according to the computations of ref. [2]. To be more specific, we want to reproduce the power law spectrum observed today

$$T(\nu) = T_{CMB} + \xi T_R \left(\frac{\nu}{\nu_0} \right)^\beta \quad (17)$$

with the parameters $T_{CMB} = 2.729\text{K}$, $\xi \approx 0.01$, $T_R = 1.19\text{K}$, $\nu_0 = 1\text{GHz}$, $\beta = -2.62$ which [2] claims will reproduce the EDGES result provided the radiation is generated before $z \sim 20$.

In order to estimate the present day background contribution from the nuggets we need to integrate their contribution over all redshifts from recombination down to $z \approx 20$. While the nuggets will continue to produce radiation below $z = 20$ it is only their large z contribution which contributes to 21 cm absorption and should be compared to the spectrum in expression (17). This contribution was previously estimated in [25] and is given by the integral,

$$I(\nu) = \int_{20}^{1100} \frac{2cdz}{3H(z)(1+z)} \rho_{DM} \langle \frac{\sigma}{M} \rangle \frac{dE}{d\nu dt dA} \quad (18)$$

where $\langle \frac{\sigma}{M} \rangle \sim \langle B \rangle^{-1/3}$ is the average cross-section to mass ratio of the nuggets and $\frac{dE}{d\nu dt dA}$ is the emission spectrum given in equation (7) evaluated at the redshift corrected frequency $\nu(1+z)$ and at the nugget temperature determined at a given redshift by expression (11). The factor of $2/3$ accounts for the fact that only the antiquark nuggets from (4) will be sufficiently heated to contribute to the spectrum at MHz frequencies. The intensity calculated in expression (18) is dependent on both the average baryon number $\langle B \rangle$ of the AQN population and the nugget temperature. However the resulting expression scales with the nuggets' average cross-section to mass ratio and is thus suppressed at large baryon number as $B^{-1/3}$ so that the value of T_{rec} required to match the spectrum (17) remains at the fraction of an eV scale within the allowed window for the baryon charge (3) for the nuggets.

For a given average baryon number we can solve for the T_{rec} value that reproduces the strength of the model (17) at the centre of the 21cm feature at $\nu \approx 75\text{MHz}$. The required T_{rec} as a function of baryon number is shown in Figure 1 and falls in the sub eV range across a wide range of nugget sizes. As a larger baryon number results in a smaller cross-section to mass ratio heavier nugget populations require a higher initial temperature to produce the radiation field suggested by the EDGES effect. As the maximum predicted values of T_{rec} is on the order of 0.7eV according to (15) the EDGES effect can only be fully saturated by nuggets with an average baryon number below $\langle B \rangle \lesssim 10^{29}$. Larger $\langle B \rangle$ values are not excluded by the EDGES result, but are insufficient to fully explain the observed feature.

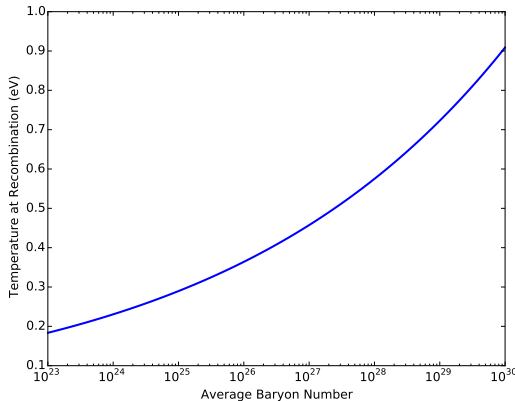


Figure 1: Nugget temperature required to produce 1% of the ARCADE2 excess as measured at $\nu = 75\text{MHz}$ as a function of the nuggets mean baryon number.

One should emphasize that this result is consistent with the window (6) derived from completely independent observations.

As may be seen in Fig. 1 matching the required sky temperature demands that the nuggets have a radiating temperature slightly below the eV scale when the universe first becomes transparent to low energy photons. As argued at the end of section 3 a precise estimate of T_{rec} is a complicated problem of the non-perturbative QCD, and highly sensitive to the microscopic details. However, we note that the lower bound on average AQN size (which is around $\langle B \rangle \sim 10^{25}$ as reviewed in Sect.2) corresponds to $T_{\text{rec}} \sim 0.3$ eV. According to expression (15) this corresponds to a lower bound on the annihilation efficiency of $\kappa \gtrsim 0.03$.

A few comments on the allowed range $1 > \kappa \gtrsim 0.03$ are in order. As argued above the value of κ is determined by a balance between the large probability of reflection at the quark nugget surface and the tendency of neutral hydrogen to lose its electron and become bound to the nugget. The case $\kappa = 1$ corresponds to a situation in which capture is completely efficient and all protons hitting the nugget annihilate. As explained above the probability for successful annihilation is expected to be strongly suppressed as it requires a perfect overlap of the wave-functions between the non-hadronic states of the colour superconductor and quarks from the proton. Within this context a suppression factor at the $\kappa \sim 0.1$ scale seems well justified, and in fact assumes a similar numerical value $\kappa_{\text{galactic}} \sim 0.1$ extracted from the analysis of the

galactic radiation excess in [51, 52], and we want to elaborate on the nature of this similarity now. The visible matter flux onto the nuggets within the galactic centre environment is similar to that discussed above at the time of recombination. Following [25, 51, 52] we may estimate the matter flux in the galactic centre as,

$$\rho_{\text{gc}} \langle v_{\text{g}} \rangle \approx 2 \times 10^9 \frac{\text{GeV}}{\text{cm}^2 \text{s}} \approx 7 \rho_{\text{vis}} \langle v \rangle |_{z=1100}, \quad (19)$$

where the estimate on the right hand side is based on equations (13) and (14). This similarity in fluxes (19) for two different environments can be directly translated into a similarity in the AQN temperatures for these two cases. An increase of the flux by factor 7 or so translates to a modest increase of the temperature (which scales as $T^{17/4}$ according to (12)) by factor of ~ 1.6 in comparison with our estimate (15).

These estimates using simple rescaling arguments should not be considered as solid predictions as there are a number of complications in the galactic environment. In particular, the galactic centre population may experience a further boost in heating due to the increased scattering cross section due to a substantial ionization fraction. The analysis of [52] found that unaccounted for diffuse radio emission from the galactic centre was saturated by the AQN contribution when $T \sim \text{eV}$ and that the global fit to galactic emissions could be improved by adding an AQN source near this scale. While subject to large uncertainties in both the dark and visible matter distribution in the galactic centre as well as the contribution of other diffuse radio sources this result is consistent with our estimate of the value of T_{rec} required to produce the 21cm feature observed by EDGES arising at a radically different epoch.

As mentioned previously, our goal is not a computation of T_{rec} , which would be an extremely difficult task involving many unknowns in strongly coupled QCD. Instead, our goal is to argue that the required value of T_{rec} which may explain the EDGES result is perfectly consistent with our previous galactic computations and with our broader understanding of how the AQN will behave in different environments. As a further consistency check we note that the estimated $T_{\text{rec}} \lesssim 0.7\text{eV}$ range (as shown in figure 1) corresponds to an average baryon number which is perfectly consistent with the window (6) for $\langle B \rangle$ derived from completely independent observations.

The spectrum which results from performing the

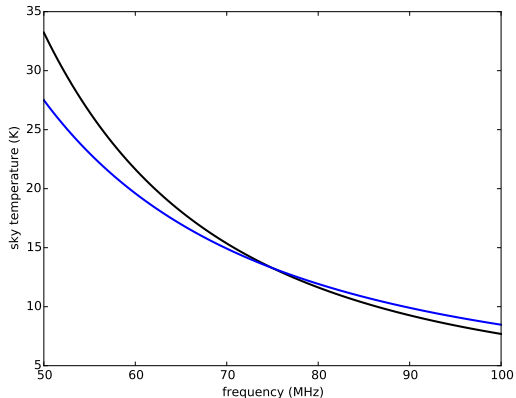


Figure 2: Sky Temperature as a function of frequency across the EDGES low-band frequency range (50-100MHz). The approximate temperature profile required to reproduce the observed 21 cm absorption feature is shown in black as is the contribution from nuggets of size $B = 10^{26}$ with the initial temperature $T_{rec} \approx 0.3\text{eV}$ chosen to match the required temperature excess 75MHz. The analysis of ref. [2] was based on formula (17) which may be reproduced by the AQN model with accuracy better than 15% across the entire relevant region.

integration of expression (18) is shown in Fig. 2 with the temperature $T_{rec} \approx 0.3\text{ eV}$ chosen to match the required sky temperature at $\nu = 75\text{MHz}$. The key observation here is that the spectrum (7) is almost constant for small frequencies at $\nu \ll T_{rec}$, while the CMB has conventional black-body suppression at small ν . This is the technical explanation why the spectrum (7) scales similarly to (17) when expressed in terms of the sky temperature.

While an additional large redshift source of radio band emission may ease the tension between present cosmological models and the EDGES result the same result limits the ionizing radiation contribution of any such source. As may be seen from the scaling in expression (16) the absorption feature will be strengthened only if the increase in radiation temperature is not accompanied by a similar increase in the ionization fraction or gas temperature. In Appendix A we present simple arguments suggesting that composite dark matter models (such as the AQN model advocated in the present work) are uniquely able to provide a radiation background of this type due to the necessary presence of dark matter at early times and the ability of composite objects to thermalize any energy produced. In conventional dark matter models (formulated in terms of local weakly interacting fields, such as WIMP

based models) the dark matter particles typically produce high energy photons or other ionizing particles which can generate a radio band signal only through subsequent interactions with the surrounding visible matter and which may significantly alter the ionization fraction.

As may be seen in Fig. 2 the spectrum of the nuggets can closely match the required radio excess with a suitable choice of initial temperature for any given average baryon number within the window (6). This is the main result of the present work. Essentially, by explicit computations within the AQN framework, we support the claim made in ref.[2] that a $\sim 1\%$ contribution to ARCADE2 excess from radiation at earlier times may explain the EDGES result. Our contribution into the field is modest: we demonstrated that the AQN model can naturally provide the required excess without conflicting with numerous strong constraints which other DM proposals face as overviewed in the Introduction.

5. Conclusion

We have argued that AQN dark matter will produce an excess of soft photons at early times. If these photons sufficiently increase the radiation temperature at long wavelengths they may produce a larger than anticipated difference between the radiation temperature and the spin temperature of the neutral hydrogen gas. This in turn, as argued in [2], will account for the stronger than anticipated 21 cm absorption feature centred at $z \approx 17$ observed by EDGES. Our computations in the AQN model should be considered as an explicit realization of the idea formulated in ref.[2] that a $\sim 1\%$ contribution to the ARCADE2 excess from radiation present at $z \sim 17$ may explain the EDGES result.

Our claim is that the AQN dark matter model is well suited to providing such a soft photon excess as the nuggets have a large number of low energy excitation levels (associated with positrons far from the nugget's surface) which will dominate their emission spectrum. In this sense the EDGES result, if confirmed, would seem to favour composite dark matter models in which any energy release may be thermalized down to the lowest available emission modes. The same composite structure of the nuggets prevents equilibration of the CMB photons with the internal temperature of the nuggets.

The technical reason for this effect to emerge is related to a very specific and unique features of the

low energy spectrum: it scales as $\ln \nu$ in eq. (7) instead of ν^3 for conventional radiation from a plasma at temperature T . This portion of the spectrum contributes very little to the total photon energy density. But this low energy portion of the spectrum could be important as a result of the Universe expansion at later times, as argued in present work.

We reiterate that this AQN model was invented as the natural explanation of the observed ratio (1), suggesting that the dark matter Ω_{dark} and the visible matter Ω_{visible} formed at the same cosmic epoch. Some of the history of this model is traced in Section 2 and the references therein. This should be contrasted with a large number of recently introduced models specifically designed to explain the EDGES result.

Acknowledgements

This research was supported in part by the Natural Sciences and Engineering Research Council of Canada.

Appendix A. Higher Energy Radiation

In this Appendix we argue that the high energy radiation which necessarily accompanies the radio band emission is negligible in the framework of the AQN dark matter model.

In particular the major portion of the energy resulting from the annihilation of a nucleus in the bulk of an AQN will be thermalized while roughly half of the near surface electron annihilations will result in the emission of a γ -ray with energy of order m_e . We may thus estimate the relative strength of thermal emission to ionizing high energy radiation as $m_p/m_e \approx 2000$.

An order of magnitude estimate of the HI ionization fraction resulting due to γ -ray emission from the nuggets demonstrates their minimal impact on gas dynamics. If we assume that every collision of an atom with an antiquark nugget results in the emission of a γ ray of average energy $E \sim m_e c^2$ then the maximum rate at which a nugget can ionize the surrounding gas is,

$$\frac{dn_{\text{ion}}}{dt} \approx \frac{m_e c^2}{I_{HI}} \frac{\rho_B}{m_p} v_B \sigma_N \quad (\text{A.1})$$

where $I_{HI} = 13.6\text{eV}$ is the ionization energy of hydrogen. Note that, as discussed in the case of nuclear annihilations, it is likely that only a fraction of

all collisions will result in an electron annihilation. This estimate is therefore an upper bound on ionizing radiation assuming all incident atoms result in a high energy photon being emitted. Scaling this expression by the antiquark nugget to hydrogen ratio,

$$\frac{n_N}{n_{HI}} = \frac{\Omega_{DM} m_p}{\Omega_B M_N} \quad (\text{A.2})$$

gives the rate of change of the ionization fraction,

$$\frac{dx_{HI}}{dt} \approx \frac{\Omega_{DM}}{\Omega_B M_N} \frac{m_e c^2}{I_{HI}} \rho_B v_B \sigma_N. \quad (\text{A.3})$$

Finally noting that $t \approx H^{-1}$ allows us to integrate this expression over redshift.

$$\begin{aligned} \Delta x_{HI} &= \int dz \frac{dt}{dz} \frac{dx_{HI}}{dt} \\ &\approx \frac{\rho_c \Omega_{DM}}{H_0 \sqrt{\Omega_M}} \frac{m_e c^2}{I_{HI}} v_0 \frac{\sigma_N}{M_N} (1 + z_{LS})^2 \end{aligned} \quad (\text{A.4})$$

where $v_0 \sim 150\text{m/s}$ is the hydrogen atom velocity scale at T_{CBM} and we have used the fact that emission is strongly peaked at early times when the universe is matter dominated. Finally, we may formulate this in terms of the average baryon number of the nuggets,

$$\Delta x_{HI} \approx 3 \times 10^{-10} \left(\frac{10^{26}}{B} \right)^{1/3}. \quad (\text{A.5})$$

Which is a negligibly small change in the ionization fraction.

Emission from the nuggets at energies $E \sim m_e c^2$ produced at $z = 1100$ will be redshifted down to the keV scale and are thus sensitive to the limits from the *Chandra* x-ray background observations [63]. However the majority of these photons are absorbed and ionize the neutral hydrogen as discussed above and the remaining x-rays are well below the observed backgrounds.

Appendix B. pre-BBN cosmology: AQN annihilation events and energy injection

In this Appendix we provide a few estimates related to energy injection during the pre-BBN cosmology when $T > 1$ MeV and the density of electrons and positrons is very high with $n_e \sim T^3$. Naively one might think that the large density of the plasma (and, therefore, frequent interactions

with the AQNs) could drastically modify the standard pre-BBN cosmology. Nevertheless, as we argue below, the main conclusion is that the corresponding rate of energy injection is negligible and does not modify the standard pre-BBN cosmology.

The basic reason for this conclusion is that the number density of the nuggets $n_{\text{AQN}} \sim B^{-1}$ is very tiny relative to the photon density due to the large baryon charge of the nuggets $B \sim 10^{25}$ and the small baryon to photon ratio $\eta \sim 10^{-10}$. The small energy injection rate, to be estimated below, is a direct consequence of this suppression factor.

We start by estimating the number of annihilation events per unit time for a single nugget. At $T > 1\text{MeV}$ annihilations are dominated by the thermally abundant electrons and positrons which may annihilate in the electrosphere bound to the AQNs. These collisions occur at a rate,

$$\frac{dN}{dt} \sim 4\pi R^2 n_e c \quad (\text{B.1})$$

where number density of electrons, positrons and photons is estimated as $n_e \sim n_{e^+} \sim n_\gamma \sim T^3$. The energy injection per unit time for a single nugget can be estimated from (B.1) by multiplying a typical energy being produced as a result of annihilation:

$$T \frac{dN}{dt} \sim 4\pi R^2 T n_e c. \quad (\text{B.2})$$

The energy injection per unit volume per unit time can be estimated as

$$\frac{dE}{dV dt} \sim 4\pi R^2 T n_{\text{AQN}} n_e c, \quad (\text{B.3})$$

where the AQN number density n_{AQN} is estimated as follows

$$n_{\text{AQN}} \sim \frac{n_B}{\langle B \rangle} \sim \eta \frac{n_\gamma}{\langle B \rangle} \sim \frac{T^3 \eta}{\langle B \rangle} \sim 10^{-35} T^3, \quad (\text{B.4})$$

where $\eta \sim 10^{-10}$ is the baryon to photon ratio. We want to estimate the total amount of energy injected into the system per unit volume during a mean free time $\tau \sim (\alpha^2 T)^{-1}$ which is defined as a typical time between collisions. The timescale τ is representative of the time needed for the system to adjust to the injected energy and return to equilibrium. We want to compare this extra injected energy (due to the AQNs) with the typical energy density in the system, i.e. we consider the dimensionless ratio

$$\frac{1}{(T n_e)} \frac{dE}{dV} \sim \frac{(R^2 T^2) \eta}{\alpha^2 \langle B \rangle} \sim 10^{-19} \left(\frac{T}{1\text{MeV}} \right)^2 \quad (\text{B.5})$$

It is clear that the small amount of energy injected into the system is quickly equilibrated within the system so that the standard pre-BBN cosmology remains intact. In other words, the conventional equation of state, and conventional evolution of the system are unaffected by presence of AQNs.

The annihilation processes of the AQNs with protons produce even smaller effect due to the additional suppression $n_B/n_e \sim \eta$ as the baryon density is drastically smaller than the electron density at $T > 1\text{MeV}$. The larger amount of energy released per collision $\sim m_p/T$ cannot overcome an additional suppression due to the very small factor $\sim \eta$. This argument, in fact, holds for much lower temperatures $T \approx 20\text{keV}$ when the number densities of protons and electrons become approximately the same order of magnitude [47].

The simple estimate presented above shows that the interaction of the AQNs with surrounding material is strongly suppressed due to the B^{-1} factor appearing in the interaction rate. The observational consequences advocated in the main body of this work emerge exclusively due to very specific and unique features of the low energy spectrum which scales as $\ln \nu$ instead of conventional ν^2 seen in the low energy tail of a blackbody spectrum. This low energy portion of the spectrum contains too little energy to effect the physics of the early universe. However, emission produced after recombination will contribute to the CMB producing a warmer than blackbody CMB spectrum at low frequencies.

References

- [1] J. D. Bowman, A. E. E. Rogers, R. A. Monsalve, T. J. Mozdzen and N. Mahesh, *Nature* **555**, no. 7694, 67 (2018).
- [2] C. Feng and G. Holder, *The Astrophysical Journal Letters*, **858** Number 2, L17, (2018) [arXiv:1802.07432](#) [astro-ph.CO].
- [3] D. J. Fixsen *et al.*, *The Astrophysical Journal*, **734** 5 (2011) [arXiv:0901.0555](#) [astro-ph.CO].
- [4] J. B. Muoz and A. Loeb, *Nature* **557**, 684 (2018). [arXiv:1802.10094](#) [astro-ph.CO].
- [5] R. Barkana, N. J. Outmezguine, D. Redigolo and T. Volansky, *Phys. Rev. D* **98**, no. 10, 103005 (2018) [arXiv:1803.03091](#) [hep-ph].
- [6] A. Fialkov, R. Barkana and A. Cohen, *Phys. Rev. Lett.* **121**, 011101 (2018) [arXiv:1802.10577](#) [astro-ph.CO].
- [7] T. R. Slatyer and C. L. Wu, *Phys. Rev. D* **98**, no. 2, 023013 (2018) [arXiv:1803.09734](#) [astro-ph.CO].
- [8] C. Li and Y. F. Cai, *Phys. Lett. B* **788**, 70 (2019) [arXiv:1804.04816](#) [astro-ph.CO].

- [9] A. Berlin, D. Hooper, G. Krnjaic and S. D. McDermott, Phys. Rev. Lett. **121**, no. 1, 011102 (2018) [[arXiv:1803.02804](#) [hep-ph]].
- [10] J. B. Muoz, C. Dvorkin and A. Loeb, Phys. Rev. Lett. **121**, 121301 (2018) [[arXiv:1804.01092](#) [astro-ph.CO]].
- [11] M. S. Mahdawi and G. R. Farrar, JCAP **1810**, no. 10, 007 (2018) [[arXiv:1804.03073](#) [hep-ph]].
- [12] E. D. Kovetz, V. Poulin, V. Gluscevic, K. K. Boddy, R. Barkana and M. Kamionkowski, Phys. Rev. D **98**, no. 10, 103529 (2018) [[arXiv:1807.11482](#) [astro-ph.CO]].
- [13] D. A. Neufeld, G. R. Farrar and C. F. McKee, Astrophys. J. **866**, no. 2, 111 (2018) [[arXiv:1805.08794](#) [astro-ph.CO]].
- [14] W. L. Xu, C. Dvorkin and A. Chael, Phys. Rev. D **97**, no. 10, 103530 (2018) [[arXiv:1802.06788](#) [astro-ph.CO]].
- [15] S. Fraser *et al.*, [[arXiv:1803.03245](#) [hep-ph]].
- [16] M. Pospelov, J. Pradler, J. T. Ruderman and A. Urbano, Phys. Rev. Lett. **121**, no. 3, 031103 (2018) [[arXiv:1803.07048](#) [hep-ph]].
- [17] S. Clark, B. Dutta, Y. Gao, Y. Z. Ma and L. E. Strigari, Phys. Rev. D **98**, no. 4, 043006 (2018) [[arXiv:1803.09390](#) [astro-ph.HE]].
- [18] A. Ewall-Wice, T.-C. Chang, J. Lazio, O. Dore, M. Seifert and R. A. Monsalve, Astrophys. J. **868**, no. 1, 63 (2018) [[arXiv:1803.01815](#) [astro-ph.CO]].
- [19] P. Sharma, Mon. Not. Roy. Astron. Soc. **481**, Issue 1,21, pages L6-L10 (2018) [[arXiv:1804.05843](#) [astro-ph.HE]].
- [20] R. Hills, G. Kulkarni, P. D. Meerburg and E. Puchwein, Nature **564**, E32-E34 (2018). [[arXiv:1805.01421](#) [astro-ph.CO]].
- [21] A. R. Zhitnitsky, JCAP **0310**, 010 (2003) [[hep-ph/0202161](#)].
- [22] X. Liang and A. Zhitnitsky, Phys. Rev. D **94**, no. 8, 083502 (2016) [[arXiv:1606.00435](#) [hep-ph]].
- [23] S. Ge, X. Liang and A. Zhitnitsky, Phys. Rev. D **96**, no. 6, 063514 (2017) [[arXiv:1702.04354](#) [hep-ph]].
- [24] S. Ge, X. Liang and A. Zhitnitsky, Phys. Rev. D **97**, no. 4, 043008 (2018) [[arXiv:1711.06271](#) [hep-ph]].
- [25] K. Lawson and A. R. Zhitnitsky, Phys. Lett. B **724**, 17 (2013) [[arXiv:1210.2400](#) [astro-ph.CO]].
- [26] E. Witten, Phys. Rev. D **30**, 272 (1984).
- [27] E. Farhi and R. L. Jaffe, Phys. Rev. D **30**, 2379 (1984).
- [28] A. De Rújula and S. L. Glashow, Nature **312**, 734 (1984).
- [29] J. Madsen, Lect. Notes Phys. **516**, 162 (1999) [[astro-ph/9809032](#)].
- [30] Y. Aoki, G. Endrodi, Z. Fodor, S. D. Katz and K. K. Szabo, Nature **443**, 675 (2006) [[hep-lat/0611014](#)].
- [31] C. Alcock and E. Farhi, Phys. Rev. D **32**, 1273 (1985).
- [32] K. van Bibber and L. J. Rosenberg, Phys. Today **59N8**, 30 (2006);
- [33] S. J. Asztalos, L. J. Rosenberg, K. van Bibber, P. Sikivie, K. Zioutas, Ann. Rev. Nucl. Part. Sci. **56**, 293-326 (2006).
- [34] Pierre Sikivie, Lect. Notes Phys. **741**, 19 (2008) [[arXiv:0610440v2](#) [astro-ph]].
- [35] G. G. Raffelt, Lect. Notes Phys. **741**, 51 (2008) [[hep-ph/0611350](#)].
- [36] P. Sikivie, Int. J. Mod. Phys. A **25**, 554 (2010) [[arXiv:0909.0949](#) [hep-ph]].
- [37] L. J. Rosenberg, Proceedings of the National Academy of Sciences **112**, 12278 (2015).
- [38] P. W. Graham, I. G. Irastorza, S. K. Lamoreaux, A. Lindner and K. A. van Bibber, Ann. Rev. Nucl. Part. Sci. **65**, 485 (2015) [[arXiv:1602.00039](#) [hep-ex]].
- [39] D. J. E. Marsh, Phys. Rept. **643**, 1 (2016) [[arXiv:1510.07633](#) [astro-ph.CO]].
- [40] A. Ringwald, PoS NOW **2016**, 081 (2016) [[arXiv:1612.08933](#) [hep-ph]].
- [41] M. M. Forbes, K. Lawson and A. R. Zhitnitsky, Phys. Rev. D **82**, 083510 (2010) [[arXiv:0910.4541](#) [astro-ph.GA]].
- [42] D. M. Jacobs, G. D. Starkman and B. W. Lynn, Mon. Not. Roy. Astron. Soc. **450**, no. 4, 3418 (2015) [[arXiv:1410.2236](#) [astro-ph.CO]].
- [43] K. Lawson and A. R. Zhitnitsky, [[arXiv:1305.6318](#) [astro-ph.CO]].
- [44] E. T. Herrin, D. C. Rosenbaum and V. L. Teplitz, Phys. Rev. D **73**, 043511 (2006) doi:10.1103/PhysRevD.73.043511 [[astro-ph/0505584](#)].
- [45] P. W. Gorham, Phys. Rev. D **86**, 123005 (2012) [[arXiv:1208.3697](#) [astro-ph.CO]].
- [46] A. Zhitnitsky, Phys. Rev. D **74**, 043515 (2006) [[astro-ph/0603064](#)].
- [47] V. V. Flambaum and A. R. Zhitnitsky, Phys. Rev. D **99**, no. 2, 023517 (2019) [[arXiv:1811.01965](#) [hep-ph]].
- [48] D. H. Oaknin and A. R. Zhitnitsky, Phys. Rev. Lett. **94**, 101301 (2005), [[arXiv:hep-ph/0406146](#)].
- [49] A. Zhitnitsky, Phys. Rev. D **76**, 103518 (2007) [[astro-ph/0607361](#)].
- [50] K. Lawson and A. R. Zhitnitsky, JCAP **0801**, 022 (2008) [[arXiv:0704.3064](#) [astro-ph]].
- [51] M. M. Forbes and A. R. Zhitnitsky, JCAP **0801**, 023 (2008) [[astro-ph/0611506](#)].
- [52] M. M. Forbes and A. R. Zhitnitsky, Phys. Rev. D **78**, 083505 (2008) [[arXiv:0802.3830](#) [astro-ph]].
- [53] A. Zhitnitsky, JCAP **1710**, no. 10, 050 (2017) [[arXiv:1707.03400](#) [astro-ph.SR]].
- [54] N. Raza, L. van Waerbeke and A. Zhitnitsky, Phys. Rev. D **98**, no. 10, 103527 (2018) [[arXiv:1805.01897](#) [astro-ph.SR]].
- [55] A. Zhitnitsky, Phys. Dark Univ. **22**, 1 (2018) [[arXiv:1801.01509](#) [astro-ph.SR]].
- [56] H. Fischer, X. Liang, Y. Semertzidis, A. Zhitnitsky and K. Zioutas, Phys. Rev. D **98**, no. 4, 043013 (2018) [[arXiv:1805.05184](#) [hep-ph]].
- [57] X. Liang and A. Zhitnitsky, Phys. Rev. D **99**, no. 2, 023015 (2019) [[arXiv:1810.00673](#) [hep-ph]].
- [58] E.N. Parker, ApJ, **264**, 642 (1983); *ibid.* **330**, 474 (1988).
- [59] J. A. Klimchuk, Solar Phys. **234**, 41 (2006) [[astro-ph/0511841](#)].
- [60] J. A. Klimchuk and Hinode Review Team, "Achievements of Hinode in the First Ten Years," 2017, PASJ, submitted [[astro-ph/1709.07320](#)].
- [61] K. Lawson, Phys. Rev. D **83**, 103520 (2011) doi:10.1103/PhysRevD.83.103520 [[arXiv:1011.3288](#) [astro-ph.HE]].
- [62] K. Lawson and A. R. Zhitnitsky, Phys. Rev. D **95**, no. 6, 063521 (2017) [[arXiv:1510.07646](#) [astro-ph.HE]].
- [63] N. Cappelluti *et al.*, Astrophys. J. **837**, no. 1, 19 (2017) [[arXiv:1702.01660](#) [astro-ph.HE]].